



OPEN

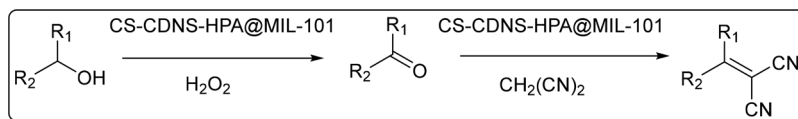
## Chitosan bead containing metal–organic framework encapsulated heteropolyacid as an efficient catalyst for cascade condensation reaction

Samahe Sadjadi<sup>1</sup>, Neda Abedian-Dehaghani<sup>2</sup>, Abolfazl Heydari<sup>3</sup> & Majid M. Heravi<sup>2</sup>

Using cyclodextrin and chitosan that are bio-based compounds, a novel bi-functional catalytic composite is designed, in which metal–organic framework encapsulated phosphomolybdic acid was incorporated in a dual chitosan-cyclodextrin nanosponge bead. The composite was characterized via XRD, TGA, ICP, BET, NH<sub>3</sub>-TPD, FTIR, FE-SEM/EDS, elemental mapping analysis and its catalytic activity was examined in alcohol oxidation and cascade alcohol oxidation–Knoevenagel condensation reaction. It was found that the designed catalyst that possess both acidic feature and redox potential could promote both reactions in aqueous media at 55 °C and various substrates with different electronic features could tolerate the aforementioned reactions to furnish the products in 75–95% yield. Furthermore, the catalyst could be readily recovered and recycled for five runs with slight loss of the catalytic activity. Notably, in this composite the synergism between the components led to high catalytic activity, which was superior to each component. In fact, the amino groups on the chitosan served as catalysts, while cyclodextrin nanosponge mainly acted as a phase transfer agent. Moreover, measurement of phosphomolybdic acid leaching showed that its incorporation in metal–organic framework and bead structure could suppress its leaching, which is considered a drawback for this compound. Other merits of this bi-functional catalyst were its simplicity, use of bio-based compounds and true catalysis, which was proved via hot filtration.

In recent decades, unprecedented rate of technological growth resulted in increase of environmental concerns<sup>1</sup>. As a solution, development of environmentally benign and practical synthetic methods that meet the criteria of green chemistry is on the agenda. In this regard, cascade reactions<sup>2</sup> that combine consecutive synthetic steps in one-pot and benefit from advantages, such as less energy consumption, less waste production and avoiding intermediate separation and purification are great tools for developing sustainable chemistry. To promote cascade reactions, multifunctional catalysts are required<sup>3</sup>, in which several catalytic active sites are introduced on a recyclable supporting material. In this context, wise choice of the support and immobilization strategy can provide synergistic effects and furnish catalysts with high efficiency. One of the well-known cascade reactions is alcohol oxidation–Knoevenagel condensation reaction that is used for the synthesis of  $\alpha,\beta$ -unsaturated nitriles. The key step in this cascade reaction is selective oxidation of alcohols to benzaldehydes, which can be catalyzed by various catalysts, such as enzymes<sup>4</sup>, metal oxides<sup>5</sup> and heteropolyacids that are non-corrosive and non-toxic inorganic metal oxide clusters<sup>6</sup> with redox potential and acidic properties. Heteropolyacids can catalyze various chemical transformations<sup>7–11</sup>, ranging from epoxidation to photo-degradations<sup>12–15</sup>. The main shortcoming of this class of inorganic clusters is their high solubility in conventional solvents that resulted in their onerous and inefficient recovery and recyclability<sup>13</sup>. As a solution to this problem, heteropolyacids have been stabilized on supporting compounds to furnish heterogeneous catalysts<sup>16</sup>. Although this strategy is helpful, leaching of heteropolyacids from the support is still a challenging issue. Knoevenagel condensation, on the other hand, can be promoted by various catalysts<sup>17–19</sup>, such as metal–organic frameworks (MOFs) and chitosan (CS)<sup>20–22</sup>. MOFs

<sup>1</sup>Gas Conversion Department, Faculty of Petrochemicals, Iran Polymer and Petrochemical Institute, P.O. Box 14975-112, Tehran, Iran. <sup>2</sup>Department of Chemistry, School of Physics and Chemistry, Alzahra University, P.O. Box 1993891176, Vanak, Tehran, Iran. <sup>3</sup>Polymer Institute of the Slovak Academy of Sciences, Dúbravská Cesta 9, 845 41 Bratislava, Slovakia. ✉email: s.sadjadi@ippi.ac.ir; mmheravi@alzahra.ac.ir



**Scheme 1.** Cascade alcohol oxidation–Knoevenagel condensation reaction.

are porous nanomaterials that are composed of metallic centers<sup>23–27</sup> and organic linkers<sup>28–30</sup> and mostly possess Lewis acidic sites. In fact, high dispersion of metal ions in the MOF frameworks allows them to interact with reagents. Other features of MOFs that make them interesting candidates for catalysis are their porous nature<sup>31</sup> and the possibility of tuning their properties through altering the linkers and metal centers<sup>32</sup>. To date various MOFs have been developed and utilized for various applications, including catalysis<sup>33–37</sup>. One of the mostly used MOFs is MIL-101(Fe), which is prepared from iron precursors and terephthalic acid and widely used for catalytic purposes<sup>38</sup>. Despite all merits of MOFs, their relatively time-consuming synthetic procedure as well as the necessity of use of toxic solvents and costly starting materials limit their large scale uses and render MOF-based catalytic systems relatively expensive. Hence, use of MOF in combination with other components to form composites can be considered as a solution<sup>39</sup>.

CS is an abundant carbohydrate<sup>40</sup> that benefits from myriad Brønsted acidic sites and Lewis basic sites in its backbone<sup>41</sup>. This carbohydrate has been extensively utilized for catalysis and to date various chemical transformations have been promoted via CS, CS-based composites and CS-beads<sup>42–45</sup>. Recently, it has been proved that CS-coated MOF could be a potential catalytic system for deacetalization–Knoevenagel cascade reaction<sup>41</sup>. Another approach for developing green and environmentally friendly methodologies, is omitting toxic solvents and promoting reactions in aqueous media that offers many economic advantages. Unfortunately, for the chemical transformations, in which hydrophobic substrates are used, immiscibility of reagents in aqueous media may cause low conversion and yield. To circumvent this issue, use of phase transfer agents, such as cyclodextrins (CDs) that are cyclic oligosaccharides with hydrophilic outer surfaces and hydrophobic cavities is suggested<sup>46–48</sup>. CDs can encapsulate the hydrophobic substrates inside their cavities and transfer them into aqueous media. Furthermore, CD-based polymeric systems, such as CD nanosponge (CDNS), are also applied for this purpose<sup>49,50</sup>. In fact, CDNSs are 3-D polymeric networks, achieved from cross-linking of CD with proper cross-linking agents, such as dimethyl carbonate and diphenyl carbonate. Compared to CD, CDNS benefits from heterogeneous nature, multiple CD units, various pores with different sizes, which allow encapsulation of various substrates<sup>51,52</sup>.

In this work, for the first time, a novel multi-task catalytic composite (CS-CDNS-HPA@MIL-101), Fig. 1, is designed and prepared that benefits from the chemistry of MOF, HPA, CDNS, and CS beads. The merits of this catalytic composite are its multi-functionality, use of bio-based components, and a small amount of HPA and MOF. The central hypothesis of our study is that the catalyst possessing both acidic and redox potential could efficiently promote alcohol oxidation and cascade alcohol oxidation–Knoevenagel condensation reactions, Scheme 1, in aqueous media under mild conditions. More importantly, the catalyst exhibited high recyclability and low HPA leaching, which makes this catalyst environmentally benign.

## Results and discussion

**Characterization of CS-CDNS-HPA@MIL-101.** The morphology of HPA@MIL-101, CDNS, and CS-CDNS-HPA@MIL-101 were evaluated with FE-SEM. Figure 2a depicts a uniform polyhedron morphology for HPA@MIL-101 with average diameter of  $2 \pm 0.4 \mu\text{m}$  that is similar to the reported value of MIL-101<sup>53</sup>. This data indicates that incorporation of low content of HPA during MIL-101 synthesis did not change the morphology of the final product. As shown in Fig. 2b, the as-prepared CDNS exhibited amorphous morphology. This observation is in good agreement with previous report<sup>54</sup>. FE-SEM images of CS-CDNS-HPA@MIL-101 (Fig. 2c, d), showed formation of beads with average diameter of  $2 \pm 0.5 \mu\text{m}$ . Additionally, FE-SEM images with high magnification confirmed that the surface of the formed beads was rough and porous.

The energy dispersive X-ray spectroscopy (EDS) and elemental mapping analyses were also carried out and demonstrated the presences of N, O, Fe, Mo, P, and C atoms in the CS-CDNS-HPA@MIL-101 (Fig. 3a). Among the detected atoms, P, O, and Mo atoms are indicative of HPA, while C, O, and N atoms are representative of CS. Furthermore, C and O atoms can be assigned to CDNS structure. Observation of Fe atom as well as O and C, is a proof for the presence of MIL-101 in the structure of the catalyst. Elemental mapping analysis, Fig. 3b, confirmed homogeneous dispersion of all atoms in CS-CDNS-HPA@MIL-101, indicating that both CDNS and HPA@MIL-101 are well-dispersed in the structure of the formed beads. The as-prepared CS-CDNS-HPA@MIL-101 consist of CS, CDNS and HPA@MIL-101.

It is well-reported that CS and CDNS prepared through melt-method are amorphous and their XRD patterns consist of a broad peak at  $2\theta = 15\text{--}25^\circ$ <sup>52,55</sup>. As shown, the characteristic peaks of HPA are the peaks at  $2\theta = 10^\circ$ ,  $26.4^\circ$ , and  $30.6^\circ$ . The wide-angle XRD pattern of MIL-101 exhibited the characteristic peaks at  $2\theta = 9.3^\circ$ ,  $9.9^\circ$ ,  $16.3^\circ$ ,  $18.7^\circ$ ,  $21.9^\circ$ ,  $26.8^\circ$  and  $28.1^\circ$ . According to the literature, MIL-101 also shows a peak at  $2\theta = \sim 2^\circ$  in low-angle XRD<sup>56</sup>. Wide-angle XRD pattern of HPA@MIL-101, Fig. 4B, is identical to that of MIL-101<sup>53</sup> and showed the characteristic peaks at  $2\theta = 9.3^\circ$ ,  $9.9^\circ$ ,  $13.0^\circ$ ,  $16.6^\circ$ ,  $18.6^\circ$ ,  $21.6^\circ$ ,  $25.8^\circ$  and  $28.1^\circ$ <sup>57</sup>. In the low-angle XRD pattern of this sample, the characteristic peak at  $2\theta = \sim 2^\circ$  is assigned to the MIL-101. In fact, as a result of low content of HPA as well as its high dispersion, HPA characteristic peaks were not observed in the XRD pattern of HPA@

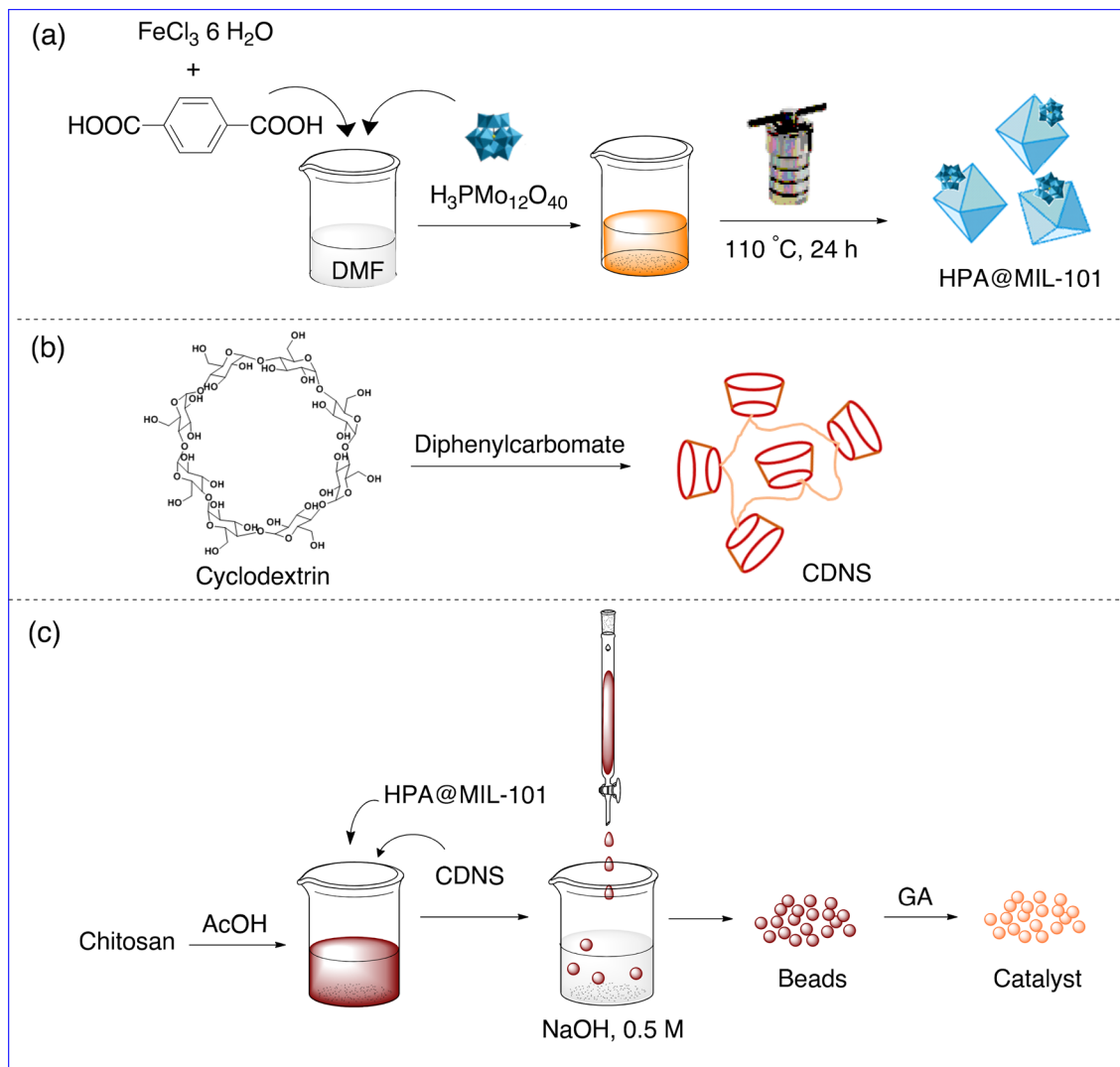


**Figure 1.** Pictorial procedure for the preparation of (a) HPA@MIL-101, (b) CDNS, and (c) CS-CDNS-HPA@MIL-101.

MIL-101<sup>58</sup>. As shown in Fig. 4B, in the wide-angle XRD pattern of CS-CDNS-HPA@MIL-101, a broad peak in the range of  $2\theta = 14\text{--}25^\circ$  was discerned and the characteristic peaks of HPA@MIL-101 were not detected. Moreover, the low-angle XRD pattern of the catalyst, Fig. 4A, indicated the disappearance of the characteristic peak at  $2\theta = \sim 2^\circ$ . According to the literature, when MOF is incorporated with another component to form a composite, the intensity of the characteristic peaks of MOF can be reduced<sup>59</sup> or even the peaks can be undetectable<sup>56,60</sup>.

To confirm formation of HPA@MIL-101 and the catalyst, their FTIR spectrum was recorded and compared with that of CS, HPA, MIL-101 and CDNS (Fig. 4). The characteristic bands of CS appeared at  $3446\text{ cm}^{-1}$  ( $-\text{OH}$ ),  $2868\text{ cm}^{-1}$  ( $-\text{CH}_2$ ),  $1388\text{ cm}^{-1}$  and  $1649\text{ cm}^{-1}$  ( $-\text{C}-\text{O}$ ). FTIR spectrum of MIL-101 exhibits the absorbance band at  $1422$ ,  $1591$  and  $1651\text{ cm}^{-1}$  that are assigned to the asymmetric and symmetric stretching modes of the  $\text{O}-\text{C}=\text{O}$  framework<sup>38</sup>. The FTIR spectrum of the as-prepared CDNS (Fig. 4) is in good agreement with the literature and exhibited the absorbance bands at  $3378\text{ cm}^{-1}$  ( $-\text{OH}$ ),  $2930\text{ cm}^{-1}$  ( $-\text{CH}_2$ ),  $1649\text{ cm}^{-1}$  ( $-\text{C}-\text{O}$ ) and  $1739\text{ cm}^{-1}$  ( $-\text{C}=\text{O}$ )<sup>38</sup>. In the FTIR spectrum of HPA, the absorbance bands detected at  $1062\text{ cm}^{-1}$  and  $956\text{ cm}^{-1}$  are ascribed to  $\text{P}-\text{O}$  and  $\text{Mo}-\text{O}$  vibration respectively. The band observed at  $847\text{ cm}^{-1}$  is assigned to the  $\text{Mo}-\text{O}-\text{Mo}$  vibration<sup>61</sup>. The absorbance bands of HPA@MIL-101 appeared at  $1413$ ,  $1595$  and  $1660\text{ cm}^{-1}$  that are assigned to the asymmetrical and symmetrical stretching modes of  $\text{O}-\text{C}=\text{O}$  and  $1388\text{ cm}^{-1}$  that is assigned to the aromatic carbon  $\text{C}-\text{C}$  vibrational mode<sup>53</sup>. It is worth mentioning that the characteristic bands observed at  $1058\text{ v}(\text{P}-\text{Oa})$ ,  $948\text{ v}(\text{Mo}-\text{Od})$ ,  $885\text{ v}(\text{Mo}-\text{Ob}-\text{Mo})$ , and  $750\text{ cm}^{-1}\text{ v}(\text{Mo}-\text{Oc}-\text{Mo})$  can be attributed to HPA, which is reported previously<sup>62</sup>. In the FTIR spectrum of CS-CDNS-HPA@MIL-101, all characteristic bands of the composite components were discerned, while some of them overlapped together.

The thermal behavior of HPA@MIL-101 and CS-CDNS-HPA@MIL-101, was evaluated using TG analysis and compared with that of CS and CDNS (Fig. 5). The thermogram of CS exhibited two weight losses at around  $100^\circ\text{C}$ , dehydration, and  $300^\circ\text{C}$ , CS backbone degradation. CDNS thermogram showed two weight losses due to dehydration at  $\sim 100^\circ\text{C}$  and CDNS degradation at  $350^\circ\text{C}$ , which are in good agreement with the literature<sup>51</sup>. In the HPA@MIL-101 thermogram, loss of water at  $\sim 100^\circ\text{C}$  was observed. The weight loss detected at  $\sim 300^\circ\text{C}$

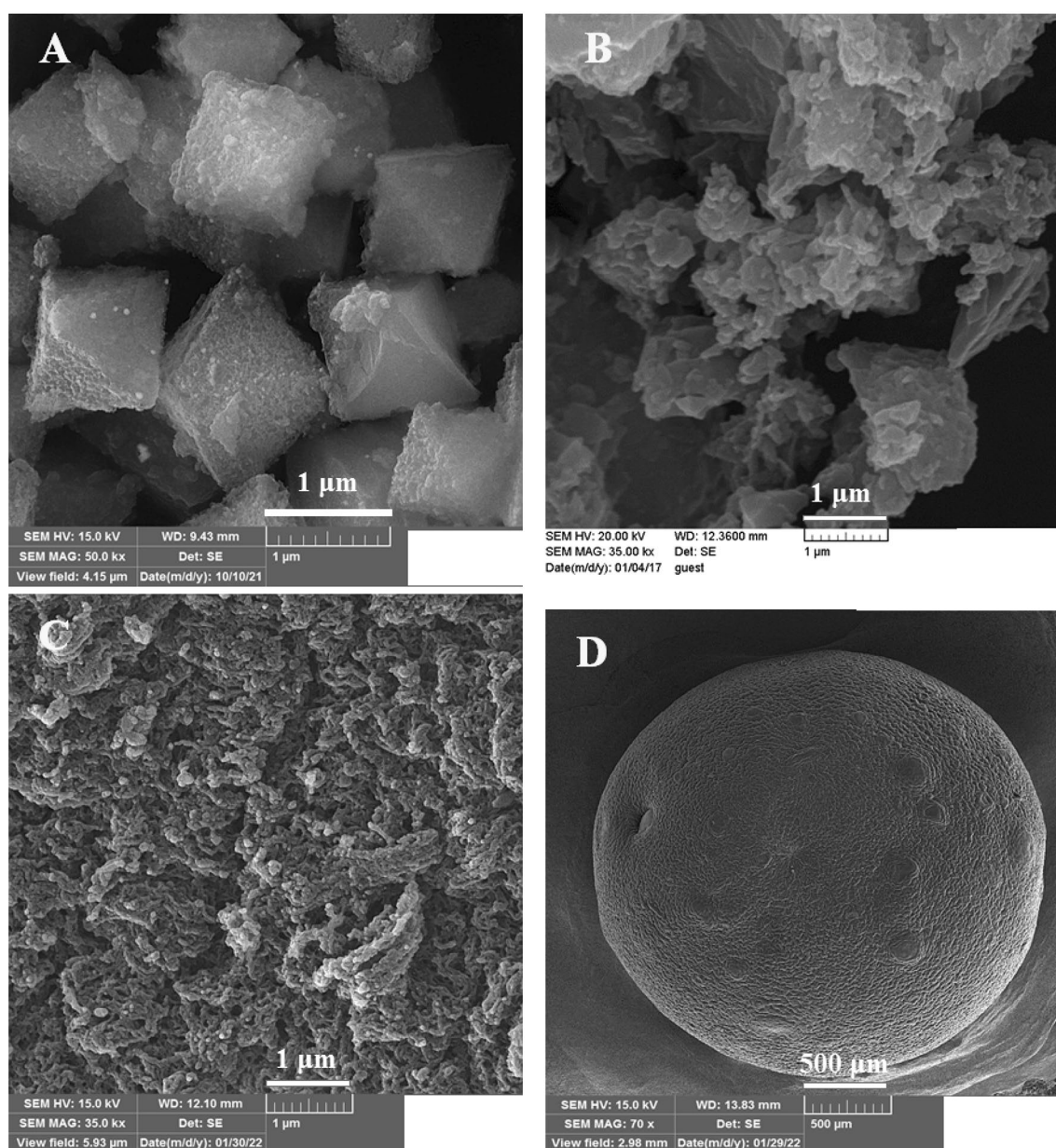


**Figure 2.** FE-SEM images of (a) HPA@MIL-101, (b) CDNS, (c) and (d) CS-CDNS-HPA@MIL-101.

can be attributed to the decomposition of the organic linkers in the structure of MOF. Figure 5 shows two weight loss steps in the thermogram of CS-CDNS-HPA@MIL-101 related to the loss of water at  $\sim 100$  °C and degradation of organic moiety (65 wt.%), i.e., CS, CDNS and the organic linkers of MOF at 200–350 °C.

$\text{NH}_3$ -TPD was applied to elucidate the acidity characteristic of CS-CDNS-HPA@MIL-101. The literature shows<sup>63</sup> that acidic sites with different strength can be classified according to the temperature of desorbed  $\text{NH}_3$  peaks. In more detail, the corresponding peaks of weak, moderate and strong acidic sites appear at 100–330, 300–450 and  $> 450$  °C respectively. In the  $\text{NH}_3$ -TPD profiles of CS-CDNS-HPA@MIL-101, two peaks were detected, one in the range of 300–600 °C that is representative of moderate to strong acidic sites and another one in the range of 650–750 °C that is indicative of strong acidic sites (Table 1). As listed in Table 1, total acidity in the catalyst was 4900 mmol/g cat.

Measurements of the textural properties of the catalyst are presented in Fig. 6. The specific surface area and pore diameter of the catalyst were  $\sim 9$   $\text{m}^2\text{g}^{-1}$  and 2.4 nm, respectively. Low specific surface area is not beyond our expectations due to the presence of chitosan in the structure of the composite, which has a very low specific surface area ( $\sim 4$   $\text{m}^2\text{g}^{-1}$ ). Specific surface area as well as other parameters, such as particle size, dispersion of the active catalytic species, the strength of the catalytic species and the number of the active sites on the catalyst can affect the catalytic activity. In fact, in determining the catalytic activity of a catalyst mostly more than one factor can be effective. The present catalyst is composed of  $\text{H}_3\text{PMo}_{12}\text{O}_{40}$ @MIL-101(Fe) in the CDNS-CS bead and more precisely, the main part of the catalyst is chitosan. Notably, the specific surface area of chitosan is low, however, the catalytic activity of chitosan for many organic transformation is high<sup>64</sup>. This issue can be due to the various

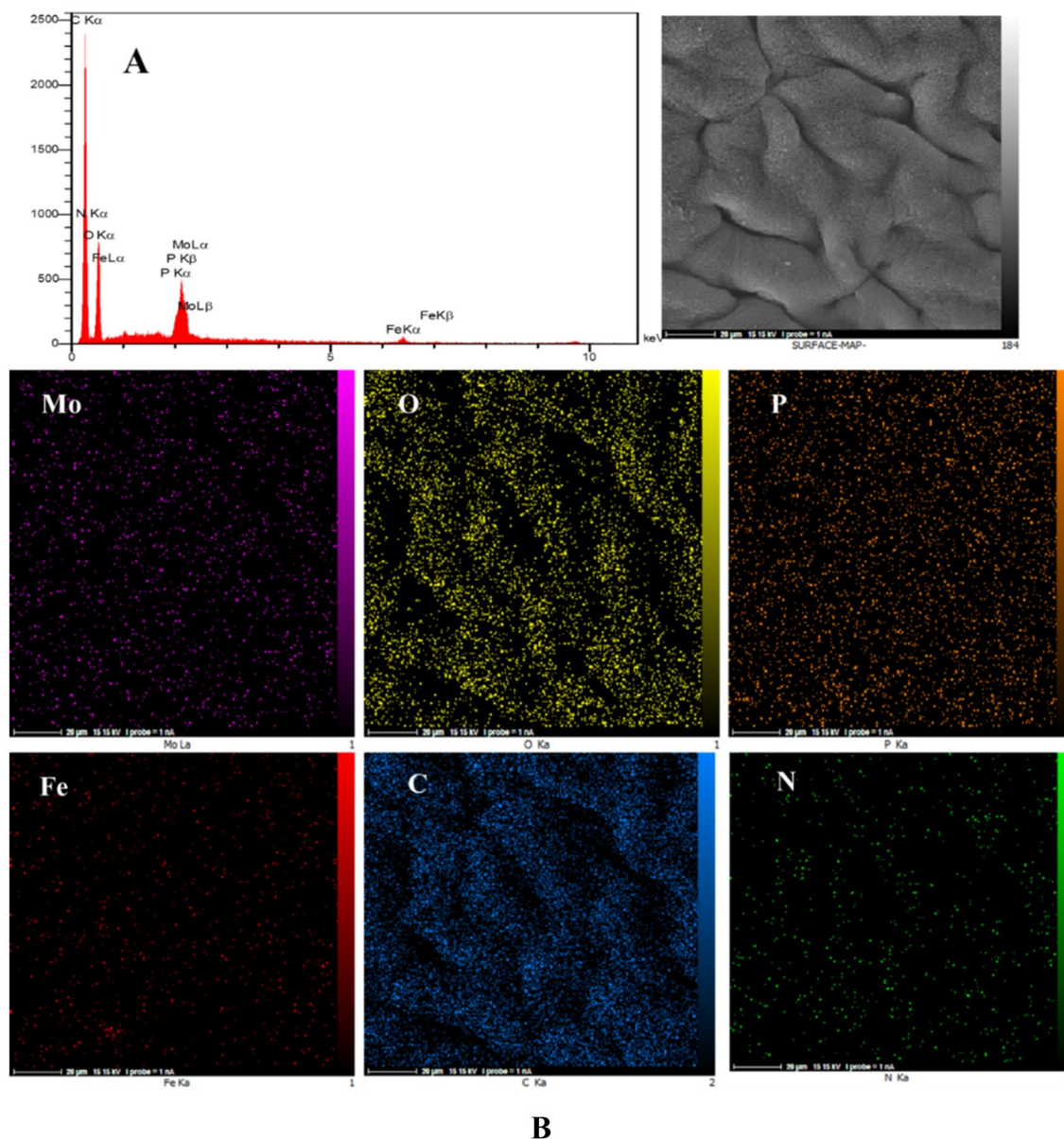


**Figure 3.** (A) EDS and (B) elemental mapping analysis of the catalyst (CS-CDNS-HPA@MIL-101).

catalytic active sites on chitosan. In other word, the specific surface area is not the only determining factor on the catalytic activity. In this catalyst, the presence of MOF and HPA that is a potent catalytic species, their good dispersion and also the presence of CDNS that is a well-known phase transfer catalyst and chitosan, which is a well-established catalyst can justify high activity of the catalyst.

**Catalytic activity of CS-CDNS-HPA@MIL-101.** *Optimization of the reaction parameters.* The main goal of our study was to promote alcohol oxidation and alcohol oxidation-Knoevenagel condensation reaction in aqueous media by designing a novel bi-functional catalyst, CS-CDNS-HPA@MIL-101. In this regard, we hypothesize that HPA with both acidic and redox potentials can promote alcohol oxidation reactions. Moreover, HPA and CS can catalyze Knoevenagel condensation reaction. In addition, CDNS was used in the catalyst structure, as a phase transfer agent, to facilitate reaction in aqueous media. It should be noted that the incorporation of HPA@MIL-101 into the bead could suppress HPA leaching.

First, alcohol oxidation was targeted and the reaction variables, including the amount of CS-CDNS-HPA@MIL-101 catalyst, oxidant content, reaction temperature and the nature of the solvent were optimized to achieve the highest conversion and yield. In this context, oxidation of benzyl alcohol was selected as a model oxidation reaction for performing optimization experiments.

*Effect of catalyst amount.* To study the effect of the catalyst loading, the model reaction was repeated in the presence of various dosages of CS-CDNS-HPA@MIL-101 and the progress of each reaction was monitored

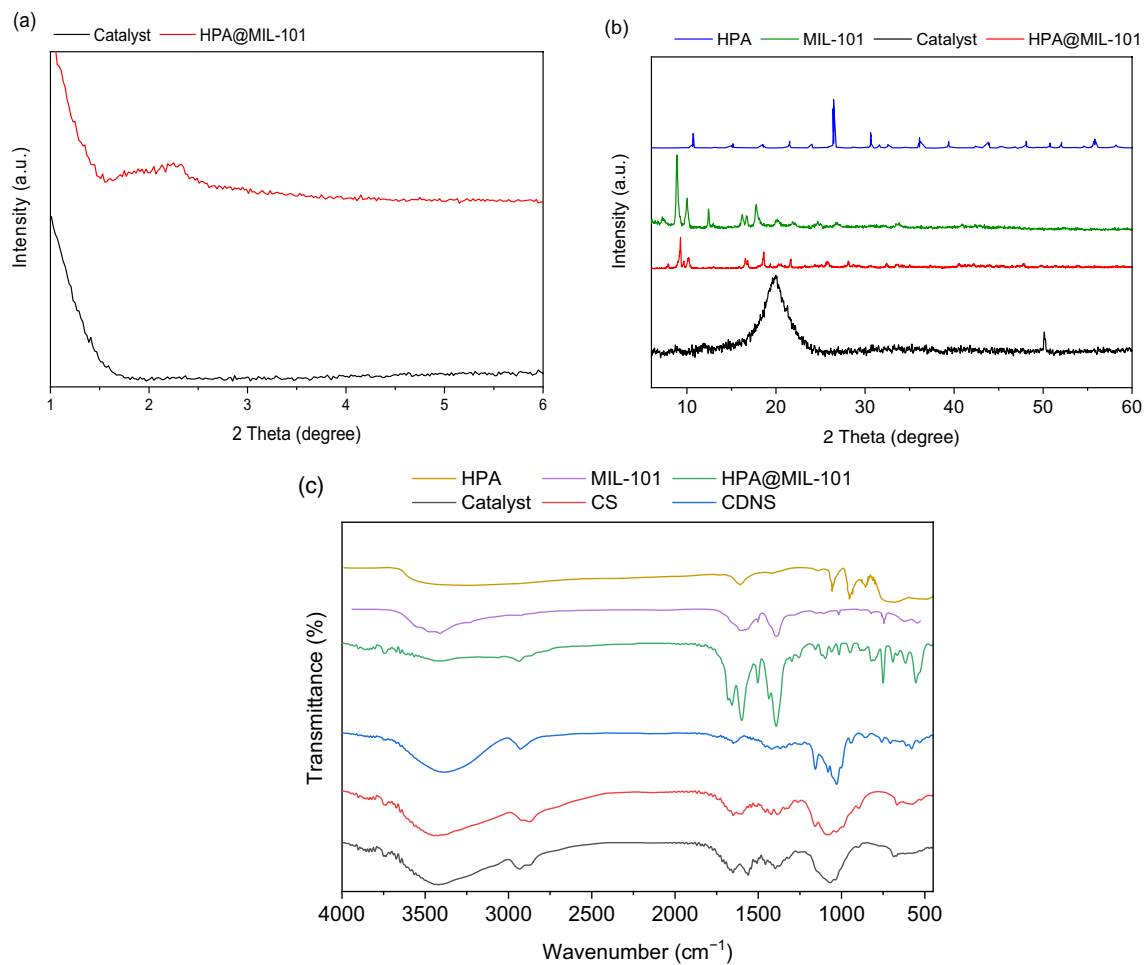


**Figure 4.** (a) Low-angle XRD patterns of HPA@MIL-101 and the catalyst (CS-CDNS-HPA@MIL-101), (b) wide-angle XRD patterns of HPA, MIL-101, HPA@MIL-101 and the catalyst, and (c) FTIR spectra of CS, HPA, MIL-101, CDNS, HPA@MIL-101, and the catalyst (CS-CDNS-HPA@MIL-101).

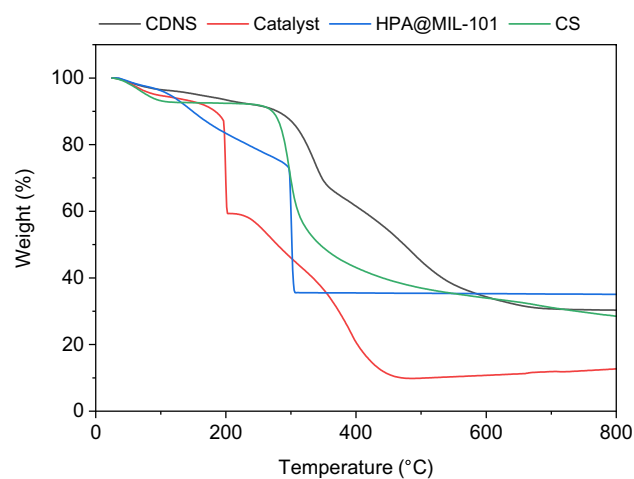


**Figure 5.** TG curves of CDNS, CS, HPA@MIL-101, and the catalyst (CS-CDNS-HPA@MIL-101).

Catalyst	Peak <sup>a</sup>	Acidity <sup>b</sup>	Peak <sup>a</sup>	Acidity <sup>b</sup>	Total acidity (mmol/g cat)
CS-CDNS-HPA@MIL-101	469	2584	470	2316	4900

**Table 1.** NH<sub>3</sub>-TPD result for the catalyst (CS-CDNS-HPA@MIL-101). <sup>a</sup>NH<sub>3</sub> peak position. <sup>b</sup>Acidity amounts (NH<sub>3</sub>/Cat, μmol·g<sup>-1</sup>).

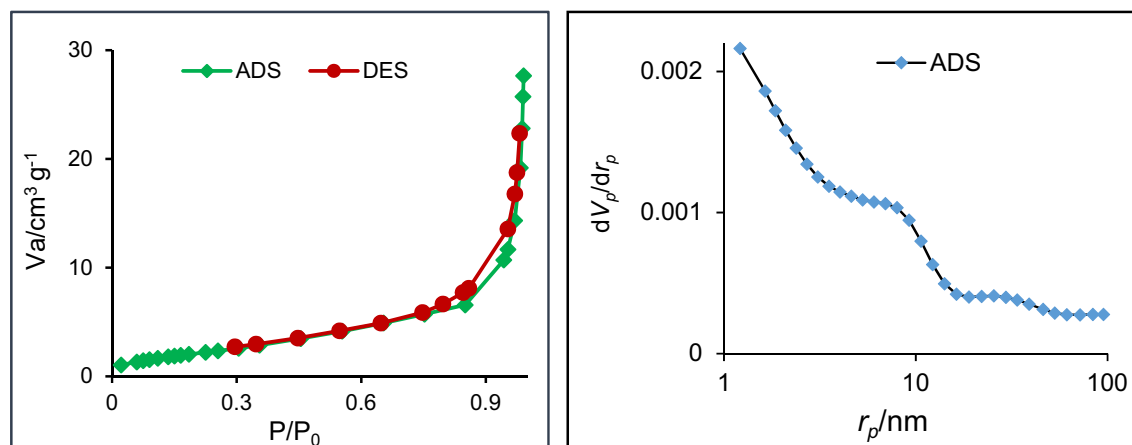


**Figure 6.** N<sub>2</sub> adsorption–desorption isotherm (left) and BJH plot (right) of the catalyst.

precisely, Fig. 7. Comparison of the conversions of the reactions implied that increase of CS-CDNS-HPA@MIL-101 content from 20 to 30 mg, led to slight increase of the reaction conversion. However, further increase of the catalyst content to 40 mg resulted in more pronounced increment of the reaction conversion. This trend was followed upon increase of this parameter to 60 mg and the reaction conversion reached to 90% after 75 min. Further increase of CS-CDNS-HPA@MIL-101 loading to 70 mg, however, had insignificant effect on the reaction conversion. More precisely, at the start of the reaction, conversion in the presence of 70 mg catalysts was ~2% higher than that of 60 mg catalyst, however, after 60 min, similar conversions were observed for the reactions in the presence of 60 and 70 mg CS-CDNS-HPA@MIL-101. Considering these results, the optimum amount of CS-CDNS-HPA@MIL-101 loading was selected as 60 mg per 1 mmol of the substrate.

*Effect of oxidant content.* Next, the amount of the oxidant, H<sub>2</sub>O<sub>2</sub>, was optimized by studying the effect of different amounts of the oxidant (0.5–3 mmol) on the conversion of the catalyst, Fig. 8. As displayed, use of low content of the oxidant (0.5 mmol) led to low conversion. Upon increase of the oxidant amount from 0.5 to 2 mmol, the reaction conversion improved gradually to reach 90% after 75 min. It is worth noting that further increase of this value to 3 mmol had a detrimental effect on the reaction conversion. Actually, use of high content of oxidant promoted oxidation of benzyl alcohol to benzoic acid. According to these experiments, the optimum value for the oxidant amount was 2 mmol per each mmol of the substrate.

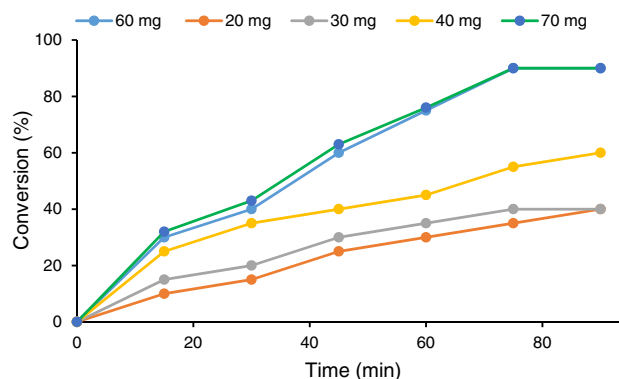


**Figure 7.** Screening the effect of the catalyst loading on the conversion of the model alcohol oxidation reaction. The reaction was performed using water as solvent and 2 mmol H<sub>2</sub>O<sub>2</sub> at 55 °C.

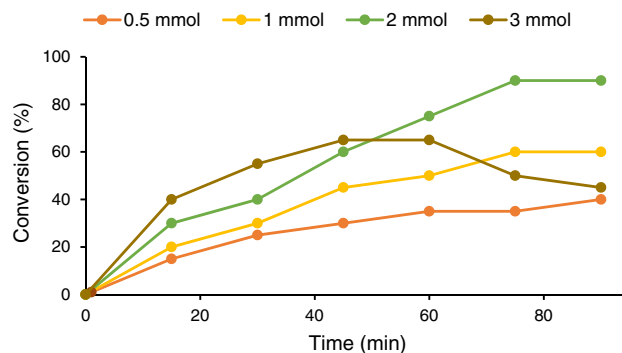


**Figure 8.** Screening the effect of oxidant amount on the conversion of the model alcohol oxidation reaction. The reaction was performed using water as solvent and 60 mg CS-CDNS-HPA@MIL-101 at 55 °C.

**Effect of reaction temperature.** The reaction temperature is another important parameter that is optimized in this work. Figure 9 shows the conversions of the model reactions at different temperatures, ambient temperature (25 °C) to 70 °C. These data indicated that increase of the reaction temperature from ambient temperature (25 °C) to 55 °C increased the reaction conversion remarkably. However, as further increase of this parameter led to the oxidation of benzyl alcohol to benzoic acid, lower yield of benzaldehyde was observed. In fact, the results confirmed that both reaction temperature and the amount of the oxidant could affect the selectivity of alcohol oxidation and their optimization is imperative to reach high conversion towards formation of aldehyde.

**Effect of reaction solvent.** As mentioned, with the goal of designing a catalyst that could promote alcohol oxidation and alcohol oxidation-Knoevenagel condensation in aqueous media, CDNS was incorporated in the structure of the catalyst to serve as a phase transfer agent. Hence, the activity of the model reaction was first examined in water as solvent. The result showed that in the aqueous media and using 60 mg CS-CDNS-HPA@MIL-101 catalyst and H<sub>2</sub>O<sub>2</sub> (2 mmol), at 55 °C, 90% conversion of the desired product was obtained. Notably, using EtOH that is a protic solvent, similar results were observed. The performance of the catalyst was also studied in THF and CH<sub>3</sub>CN and it was found that in those aprotic solvents, lower conversions and yields were achieved. The data are summarized in Table S1.

**Generality study.** The optimization experiments confirmed that CS-CDNS-HPA@MIL-101 could efficiently promote the model alcohol oxidation reaction under the optimum reaction conditions. To confirm the generality of the developed protocol, examining of other substrates with different properties was imperative. As listed in Table S2, various alcohols with different electronic and steric properties could undergo oxidation reaction under the optimum reaction conditions to furnish the corresponding aldehydes in high to excellent yields. Comparison of the yields of the substrates, indicated that oxidation of aliphatic substrates was less efficient than benzyl alcohol derivatives. Moreover, it was observed that the presence of the electron-withdrawing functional groups on the aromatic ring was beneficiary and higher yields were achieved in the cases of substrates with less electronic density.

**Alcohol oxidation-Knoevenagel condensation.** Confirming high catalytic activity of CS-CDNS-HPA@MIL-101 for alcohol oxidation reaction, its performance for the cascade oxidation-Knoevenagel condensation reaction

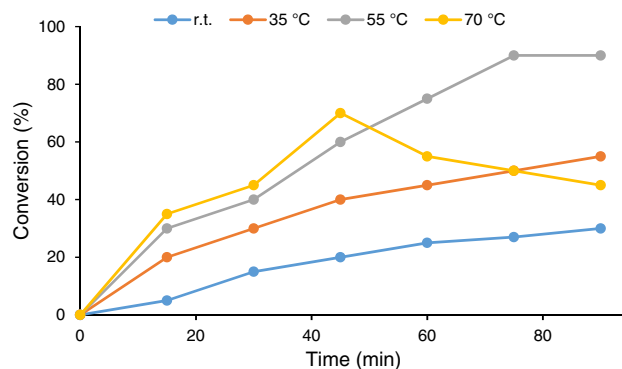


**Figure 9.** Screening the effect of temperature on the conversion of the model alcohol oxidation reaction. The reaction was performed using water as solvent, 60 mg CS-CDNS-HPA@MIL-101 and 2 mmol H<sub>2</sub>O<sub>2</sub>.



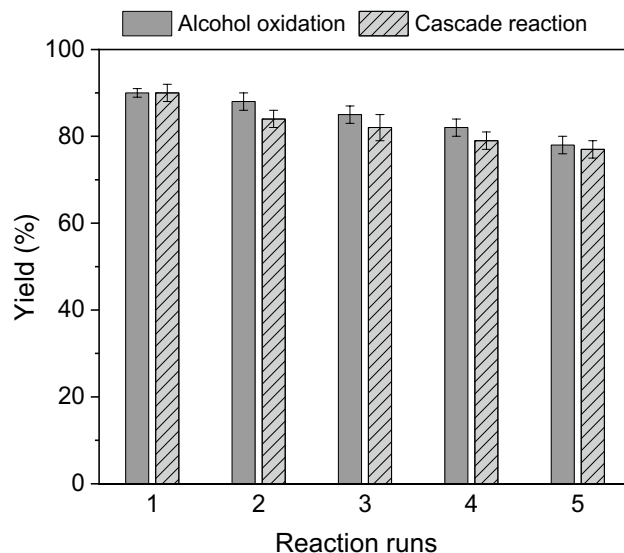
was also studied. In fact, it was assumed that the redox potential of the catalyst could promote alcohol oxidation reaction, while the presence of CS and CDNS as well as the acidic characteristic of HPA@MIL-101 could catalyze Knoevenagel condensation reaction. To validate this assumption, cascade oxidation-Knoevenagel condensation reaction of benzyl alcohol and malononitrile was first conducted under the aforesaid optimum conditions. Gratifyingly, it was found that under the so-called conditions, the desired product was achieved in 90% yield. Motivated by this result, cascade oxidation-Knoevenagel condensation reaction of various alcohols was carried out to assay the generality of this protocol, Table S3. As tabulated, various alcohols with different steric and electronic characteristic tolerated this cascade reaction to give the corresponding product in high to excellent yields. Similar to the alcohol oxidation reaction, the presence of aromatic ring on the backbone of the substrate led to the higher yields of the products.

**Control catalysts.** HPA in the structure of CS-CDNS-HPA@MIL-101 possesses redox potential and was utilized for catalyzing alcohol oxidation. To render HPA heterogeneous, it was encapsulated in MIL-101 and the resultant HPA@MIL-101 was then included in the CS-CDNS bead structure. In fact, it was postulated that interactions between HPA@MIL-101 and the functional groups on CS and CDNS can contribute to embed HPA@MIL-101 in the bead structure. In catalyst design, two roles were perceived for CDNS, as a phase transfer agent and as a bio-based catalyst for promoting Knoevenagel condensation. In more detail, encapsulation of hydrophobic substrates in the CDNS pores can facilitate their transferring to aqueous media and consequently enhance the reaction yield. On the other hand, the multiple –OH functionalities on CDNS can activate the substrate and promote Knoevenagel condensation. Another reason for incorporation of HPA@MIL-101 in CS-CDNS bead was the catalytic nature of CS and its potential for promoting Knoevenagel condensation. Furthermore, the cross-linked CS-CDNS beads were robust and could be easily separated from the reaction media. Notably, it was assumed that possible synergistic effects among the composite components can improve the catalytic activity of the composite compared to individual components. To validate the aforementioned assumptions, several control catalysts (HPA@MIL-101, CS-HPA@MIL-101, CDNS-HPA, CS-HPA, CS-CDNS-HPA) have been prepared and their activity for the model alcohol oxidation-Knoevenagel condensation reaction was examined under the optimum reaction conditions. The results, Table 2, designated that under the aforementioned conditions, CS-HPA and CDNS-HPA could catalyse the reaction to furnish the desired alcohol oxidation-Knoevenagel condensation product in 55% and 45% yield respectively. It is supposed that apart from HPA, the functionalities on CS and CDNS can participate in the catalysis. Next, to investigate the role of MIL-101 in the catalysis, a MIL-101-free control catalyst, CS-CDNS-HPA, was prepared and examined for the model alcohol oxidation-Knoevenagel condensation reaction. As shown in Table 2, the catalytic activity of this sample was higher than the aforesaid control catalyst and lower than that of CS-CDNS-HPA@MIL-101, confirming the role of MIL-101 in the catalysis. To further affirm contribution of MIL-101 to the catalysis, HPA@MIL-101 control catalyst was prepared and its activity for the model reaction was appraised. As listed, using this control catalyst, moderate reaction yield (65%) was achieved that was higher compared to CS-HPA, CDNS-HPA and CS-CDNS-HPA. This observation showed that MIL-101 not only is a potent support, but also can contribute to the catalysis. To demonstrate the role of CDNS in the catalysis, a CDNS-free control catalyst, CS-HPA@MIL-101, was examined for the model reaction and the result showed that this catalyst led to the desired product in 70% yield. As the activity of this control catalyst was lower than that of CS-CDNS-HPA@MIL-101, it can be deduced that CDNS play an important role in the catalysis. As mentioned before, the main role of CDNS is shuttling the substrates in the aqueous media. Noteworthy, the catalytic activity of all of the aforementioned control catalysts was inferior to that of CS-CDNS-HPA@MIL-101, confirming that hybridization of CS, CDNS and HPA@MIL-101 is beneficiary for the catalysis.

**Recyclability of CS-CDNS-HPA@MIL-101.** Recyclability of a heterogeneous catalyst is an important feature, determining its potential for commercial and large-scale uses. Considering high solubility of HPA in conventional solvents, some HPA-based heterogeneous catalyst showed poor recyclability. To appraise the recyclability of CS-CDNS-HPA@MIL-101, its performance for five consecutive runs for both model alcohol oxidation and cascade alcohol oxidation-Knoevenagel condensation reactions under the optimum conditions was evaluated. To this purpose, after the first run of the reaction the catalyst was separated, washed with EtOH and dried at 70 °C overnight. Then the recovered catalyst was reused for the next reaction run. As shown in

Entry	Catalyst	Yield (%)
1	CS-CDNS-HPA@MIL-101	90
2	CS-HPA	55
3	CDNS-HPA	45
4	CS-CDNS-HPA	61
5	HPA@MIL-101	65
6	CS-HPA@MIL-101	70

**Table 2.** The activity of the control catalysts and CS-CDNS-HPA@MIL-101 for the model alcohol oxidation-Knoevenagel condensation reaction. Reaction conditions: alcohol (1 mmol), H<sub>2</sub>O<sub>2</sub> (30%, 0.6 mmol) and CS-CDNS-HPA@MIL-101 (60 g) were mixed in H<sub>2</sub>O (7 mL) and then, malononitrile (1.2 mmol) was added and the reaction was proceeded at 55 °C for 1.5 h.



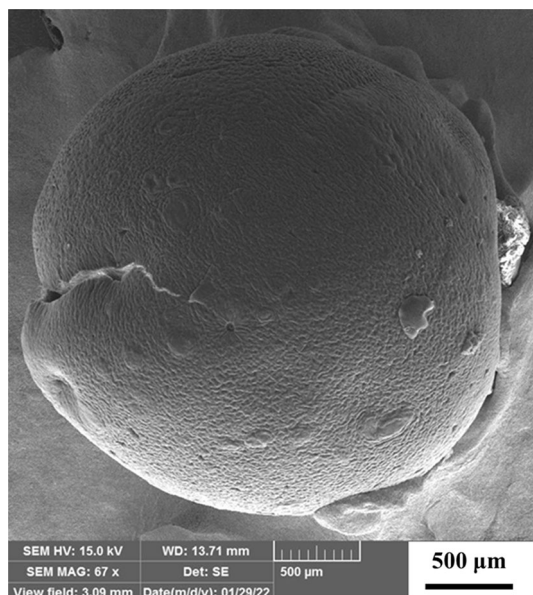
**Figure 10.** Recyclability of CS-CDNS-HPA@MIL-101 for the model alcohol oxidation and cascade alcohol oxidation-Knoevenagel condensation reaction. Reaction conditions for alcohol oxidation reaction: mixing of alcohol (1 mmol), CS-CDNS-HPA@MIL-101 (60 mg) and  $\text{H}_2\text{O}_2$  (2 mmol) at 55 °C. Reaction conditions for cascade alcohol oxidation-Knoevenagel condensation reaction: alcohol (1 mmol),  $\text{H}_2\text{O}_2$  (30%, 0.6 mmol) and CS-CDNS-HPA@MIL-101 (60 g) were mixed in  $\text{H}_2\text{O}$  (7 mL) and then, malononitrile (1.2 mmol) was added and the reaction was stirred at 55 °C for 1.5 h.

Fig. 10, for both reactions, slight loss of the catalytic activity was observed upon each run of recycling and the reaction conversion decreased from 90 to 78% for benzyl alcohol oxidation reaction and 90–77% for cascade benzyl alcohol oxidation-Knoevenagel condensation reaction on the fifth run of the reactions.

To assay the origin of loss of the activity of CS-CDNS-HPA@MIL-101 upon recovery-reuse cycle, the recovered catalyst after the fifth run of alcohol oxidation-Knoevenagel condensation was analysed via FTIR spectroscopy. In the FTIR spectrum of the recycled CS-CDNS-HPA@MIL-101, Figure S1, the distinguished absorbance bands of fresh CS-CDNS-HPA@MIL-101 are detectable, confirming that CS-CDNS-HPA@MIL-101 was stable upon several runs of recycling. It is worth mentioning that in the FTIR spectrum of the recycled catalyst, an additional band at  $2212\text{ cm}^{-1}$  can be discerned that is ascribed to the  $-\text{CN}$  functionality, indicating deposition of malononitrile and/or cascade reaction product on the catalyst. As the deposited chemicals can hinder the accessibility of the substrates to the active sites of CS-CDNS-HPA@MIL-101, it can play a role in deactivation of the catalyst. Another important factor that can affect the catalytic activity is leaching of HPA. To elucidate whether several runs of recycling can trigger HPA leaching, ICP analysis of the recycled CS-CDNS-HPA@MIL-101 was conducted. Gratifyingly, the leaching of HPA after five runs of recycling was insignificant (only 1 wt.% of the initial loading), implying that incorporation of HAP in the composite could efficiently suppress its leaching.

Morphological study of the recycled catalyst after five runs of the cascade alcohol oxidation-Knoevenagel condensation reaction under the optimum reaction condition, Fig. 11, indicated that even after several recovery and reusing runs, the morphology of the catalyst is similar to the fresh catalyst and the catalyst preserve its spherical morphology. However, in some cases the beads showed some cracks.

**Hot filtration test.** In the heterogeneous catalysis, two possible routes can be followed. In the first route, which is referred as true heterogeneous catalysis, the catalytic species are immobilized on the support in the course of the reaction. While in the second route, the stabilized catalytic species leaches in the reaction media during the reaction and then re-deposits on the support. Hence, to elucidate whether the catalysis is truly heterogeneous, Hot-filtration test is used<sup>65</sup>, in which the reaction is halted after a short reaction time, the catalyst is removed from the reaction media and the progress of the reaction is monitored over the time. In the case of true heterogeneous catalysis, it is expected that the reaction does not proceed after separation of the catalyst. In this study, to elucidate the nature of CS-CDNS-HPA@MIL-101 catalysis, hot filtration test was performed for both CS-CDNS-HPA@MIL-101-catalysed benzyl alcohol oxidation and the cascade alcohol oxidation-Knoevenagel condensation under the optimum reaction conditions. Monitoring of the conversion of both reactions (Figure S2) indicated that in the presence of the catalyst, the reactions proceeded to furnish 52% aldehyde after 30 min and 49% benzylidene malononitrile after 15 min. Upon removal of CS-CDNS-HPA@MIL-101 from the reaction media, no noticeable change in the conversion of both reactions was observed over the time. These findings imply the true heterogeneous nature of catalysis.



**Figure 11.** FE-SEM image of the recycled catalyst after five runs of cascade alcohol oxidation-Knoevenagel condensation reaction. Reaction conditions alcohol (1 mmol),  $\text{H}_2\text{O}_2$  (30%, 0.6 mmol) and CS-CDNS-HPA@MIL-101 (60 g) were mixed in  $\text{H}_2\text{O}$  (7 mL) and then, malononitrile (1.2 mmol) was added and the reaction was stirred at stirred at 55 °C for 1.5 h.

**Plausible mechanism for alcohol oxidation-Knoevenagel condensation.** The selected cascade reaction in our study involves two consecutive steps, alcohol oxidation and Knoevenagel condensation, which is illustrated in Fig. 12. According to the literature<sup>66</sup>, in the first step, one proton of  $\text{H}_2\text{O}_2$  is transferred to one of the oxygen atoms in the  $\text{MoO}_2$  unit in HPA and the formed  $\text{HO}_2^-$  is coordinated to the Lewis-acidic metal center to generate peroxy intermediate, which oxidizes alcohol to furnish the corresponding aldehyde and water. In the next step, the generated aldehyde takes part into the Knoevenagel condensation. In this regard, the catalyst activates malononitrile to form an activated methylene compound. Simultaneously, the catalytically active sites in the bead can activate the aldehyde to form an active intermediate, which then tolerates reaction with the as-prepared activated methylene compound to give the Knoevenagel condensation product as well as the catalyst (Fig. 12)<sup>67</sup>.

**Comparative study.** Alcohol oxidation-Knoevenagel condensation reaction is an important cascade reaction that can be applied for the synthesis of more complicated organic compounds. To date various catalysts have been developed for promoting this reaction under different reaction conditions. Table 3 summarized the performance of the model reactions with some randomly selected catalysts to assay the catalytic activity of CS-CDNS-HPA@MIL-101 in comparison with the previously reported ones. Comparison of the yield of the model product as well as the reaction conditions affirms that some catalysts are inefficient and led to scant yield of the desired product (Table 3, entries 2, 4, and 7). Although some other catalysts, such as  $\text{NH}_2$ -MIL-101(Fe) and Zr-MOF- $\text{NH}_2$  resulted in moderate to high yields of the desired product, use of organic and toxic solvents as well as long reaction time rendered them less attractive. Taking the data in Table 3 into account, the catalytic activity of CS-CDNS-HPA@MIL-101 is superior to or equivalent to the reported catalysts so far. These data confirm that the designed catalyst can be considered as an efficient catalyst for promoting alcohol oxidation-Knoevenagel condensation reactions. It is worth noting that there are defiantly some protocols that may led to the higher yields of the desired products in even milder conditions. In fact, our random comparison is just for indicating that the activity of CS-CDNS-HPA@MIL-101 is comparable with some reported catalysts.

## Experimental section

The chemicals used for this research as well as the detail of the instruments are presented in supporting information.

**Preparation of HPA@MIL-101.** To prepare HPA@MIL-101,  $\text{FeCl}_3 \cdot 6\text{H}_2\text{O}$  (7 mmol) and  $\text{H}_2\text{BDC}$  (7 mmol) were dissolved in DMF (70 mL) and mixed at ambient temperature (25 °C) for 30 min. HPA (0.12 mmol) was slowly added to the prepared solution and the mixture was stirred at ambient temperature for 2 h and then transferred into a Teflon-lined hydrothermal reactor and heated at 110 °C for 24 h. At the end, the reactor was cooled and the reaction product was isolated from solution via centrifugation. The obtained precipitate washed repeatedly with MeOH and dried in vacuum at 90 °C. ICP analysis showed that the content of HPA in HPA@MIL-101 was 6.6 wt.%.

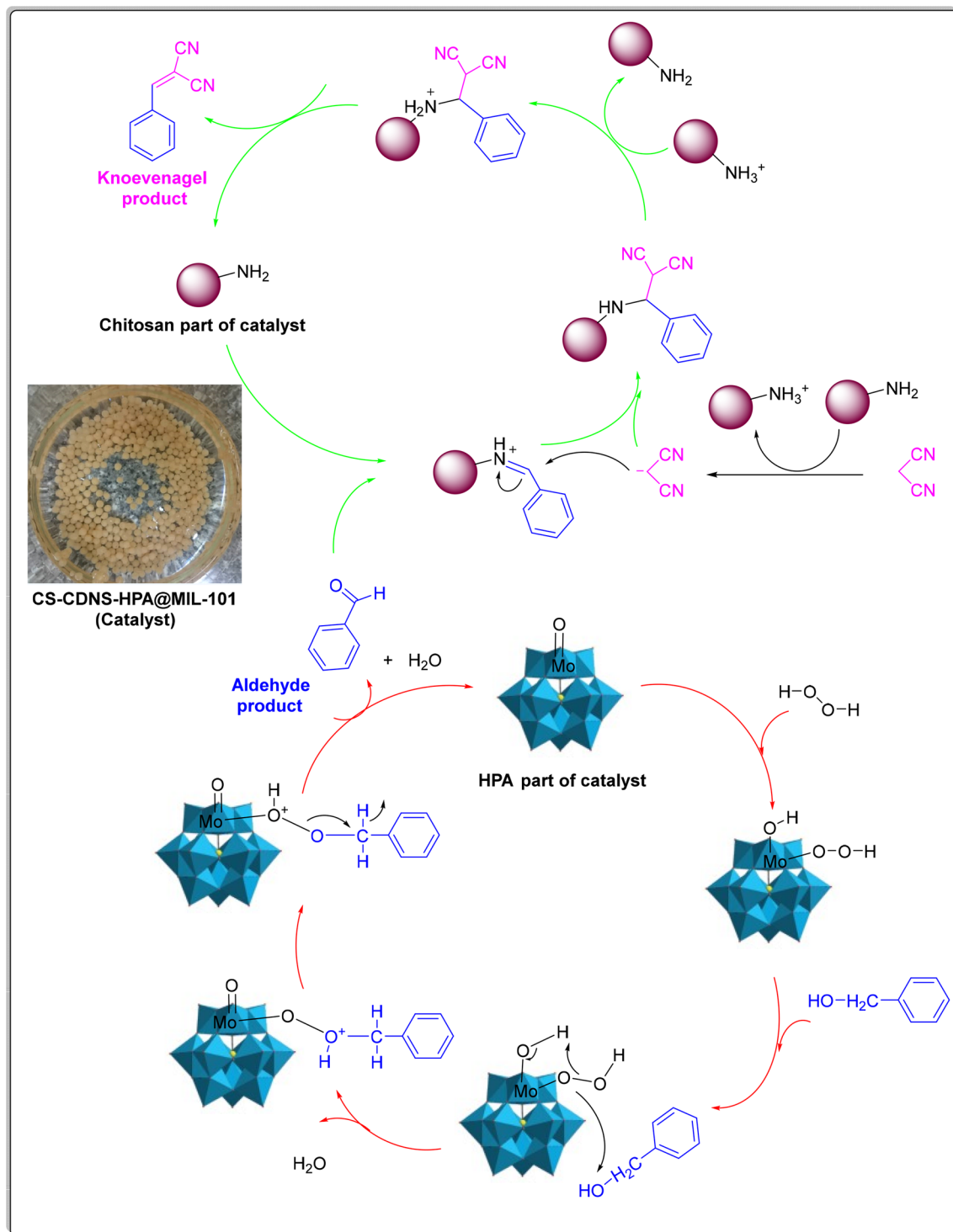


**Figure 12.** The plausible mechanism for the cascade alcohol oxidation-Knoevenagel condensation reaction highlighting the catalyst effect.

**Preparation of CDNS.** CDNS was prepared through our previously reported method<sup>51</sup>. Briefly, diphenyl carbonate (8 mmol) was added to a beaker and heated on a hot plate. Then,  $\beta$ -CD (1 mmol) was slowly added to the melted diphenyl carbonate and the mixture was stirred vigorously at 120 °C overnight to obtain a white solid. Subsequently, the beaker was cooled and the obtained CDNS was crushed to powder. Then, the prepared CDNS was purified by washing repeatedly with acetone and distilled water, followed by Soxhlet with ethanol around 12 h. The pure CDNS was then dried at ambient temperature (25 °C).

Entry	Catalyst	Catalyst amount	Reaction conditions	Time (h)	Benzylidene malononitrile (yield %)	References
1	Cu <sub>3</sub> TATAT-3 <sup>a</sup>	8 mol%	CH <sub>3</sub> CN/O <sub>2</sub> /75 °C	12	95	68
2	NH <sub>2</sub> -MIL-125(Ti)	20 mg	O <sub>2</sub> /light irradiation	40	3.3	69
3	NH <sub>2</sub> -MIL-101(Fe)	20 mg	O <sub>2</sub> /light irradiation	40	72	69
4	Ti-MOF-NH <sub>2</sub>	100 mg	<i>p</i> -Xylene/O <sub>2</sub> /UV irradiation	48	32	70
5	Zr-MOF-NH <sub>2</sub>	100 mg	<i>p</i> -Xylene/O <sub>2</sub> /UV irradiation	48	91	70
6	UoB-2 <sup>b</sup>	2 mol%	Solvent-free EtOH/TBHP	1.5	94	71
7	NH <sub>2</sub> -UiO-66(Zr)	20 mg	O <sub>2</sub> /light irradiation	40	4.6	69
8	Fe <sub>3</sub> O <sub>4</sub> @SiO <sub>2</sub> @PEI@Ru(OH) <sub>x</sub>	100 mg	O <sub>2</sub> /110 °C for alcohol oxidation step	22	90.2	72
9	CS-CDNS-HPA@MIL-101	60 mg	H <sub>2</sub> O/H <sub>2</sub> O <sub>2</sub> /55 °C	1.5	90	This work

**Table 3.** The activity of CS-CDNS-HPA@MIL-101, the designed catalyst in this work, for alcohol oxidation-Knoevenagel condensation reaction in comparison with the reported catalysts in literature. <sup>a</sup>bifunctional copper metal organic framework <sup>b</sup>Ni-based metal-organic framework.

**Preparation of CS-CDNS-HPA@MIL-101.** To prepare the composite bead, to a solution of CS (1 g) in acetic acid (50 mL, 2 w/v%), the as-prepared CDNS (0.33 g) and HPA@MIL-101 (0.33 g) were added. The mixture was stirred for 3 h to achieve a homogeneous suspension. Then, the obtained suspension was transferred into a burette and gently dropped into a solution of NaOH (0.5 mol L<sup>-1</sup>) to form fine beads and they were kept in the basic solution overnight. To covalently crosslink the beads, they were collected, rinsed with distilled water, and then introduced into a solution of GA (5 w/v% in EtOH) and stirred at 70 °C for 13 h. Finally, the covalently cross-linked beads were collected, rinsed with EtOH, and dried at ambient temperature, 25 °C (Fig. 1).

**Alcohol oxidation.** To examine the activity of CS-CDNS-HPA@MIL-101 for alcohol oxidation, alcohol (1 mmol), CS-CDNS-HPA@MIL-101 (60 mg) and H<sub>2</sub>O<sub>2</sub> (2 mmol) were mixed in H<sub>2</sub>O at 55 °C and the reaction progress was monitored by Thin-layer chromatography (TLC). Upon completion of the oxidation reaction, CS-CDNS-HPA@MIL-101 was removed from the reaction medium by centrifugation and the solvent of the filtrate was evaporated to achieve the product. The yield of the reaction was measured by gas chromatography (GC) and the separated catalyst was washed with EtOH, dried at 70 °C overnight and reused for the next reaction run.

**Cascade alcohol oxidation-Knoevenagel condensation reaction.** The activity of CS-CDNS-HPA@MIL-101 was evaluated for cascade alcohol oxidation-Knoevenagel condensation (Scheme 1). To perform the reaction, a solution of alcohol (1 mmol), H<sub>2</sub>O<sub>2</sub> (30%, 0.6 mmol) in H<sub>2</sub>O (7 mL) and CS-CDNS-HPA@MIL-101 (60 g) were placed in a round-bottomed flask and then stirred at 55 °C. Subsequently, malononitrile (1.2 mmol) was added, the reaction mixture was stirred and the progress of the reaction was monitored by TLC. Upon completion of the reaction, CS-CDNS-HPA@MIL-101 was separated and recovered by washing with EtOH and drying at 70 °C overnight. The recovered CS-CDNS-HPA@MIL-101 was used for the next run of the cascade reaction. Knoevenagel product was obtained after evaporation of the solvent and silica gel column chromatography with petroleum ether-EtOAc (5: 1), Figures S3-S12.

## Conclusions

In designing the new generation of catalyst, the multi-component catalyst benefiting from multi-functional activity addresses the requirements of green chemistry principles in a wide range of organic reactions is introduced and used for catalyzing both alcohol oxidation and cascade alcohol oxidation-Knoevenagel condensation reaction in aqueous media. We propose an easy and efficient synthesis process for the preparation of the catalyst (CS-CDNS-HPA@MIL-101). The physico-chemical characteristics of the catalyst were studied using various techniques and show a bead where the components are well-dispersed. Our finding highlights the high catalytic activity toward alcohol oxidation and cascade alcohol oxidation-Knoevenagel condensation reactions. This behavior indicates the CDNS acted mainly as a phase transfer agent, HPA served as a bifunctional catalyst with both acidic and redox potential, and amino groups on CS acted as basic catalysts. It should be noted that the encapsulation of HPA in MIL-101 and also the incorporation of HPA@MIL-101 in the structure of the bead could suppress HPA leaching and result in good recyclability of the catalyst. More importantly, the catalysis was truly heterogeneous and did not follow the leaching-deposition cycle in the course of catalysis.

## Data availability

The datasets used and/or analyzed during the current study are available from the corresponding author on reasonable request.

Received: 1 November 2022; Accepted: 6 February 2023

Published online: 16 February 2023

## References

- Sanchez-Martin, J., Gonzalez-Velasco, M., Beltran-Heredia, J., Gragera-Carvajal, J. & Salguero-Fernandez, J. Novel tannin-based adsorbent in removing cationic dye (Methylene Blue) from aqueous solution. Kinetics and equilibrium studies. *J. Hazard Mater.* **174**, 9–16. <https://doi.org/10.1016/j.jhazmat.2009.09.008> (2010).
- Huang, H.-M., Garduño-Castro, M. H., Morrill, C. & Procter, D. J. Catalytic cascade reactions by radical relay. *Chem. Soc. Rev.* **48**, 4626–4638. <https://doi.org/10.1039/C8CS00947C> (2019).
- Watson, G. *et al.* A Ru-complex tethered to a N-rich covalent triazine framework for tandem aerobic oxidation-knoevenagel condensation reactions. *Molecules* **26**, 838 (2021).
- Pothast, A., Rosenau, T., Chen, C. L. & Gratzl, J. S. A novel method for conversion of benzyl alcohols to benzaldehydes by laccase-catalysed oxidation. *J. Mol. Catal. A Chem.* **108**, 5–9. [https://doi.org/10.1016/1381-1169\(95\)00251-0](https://doi.org/10.1016/1381-1169(95)00251-0) (1996).
- Wang, F. & Ueda, W. Aerobic oxidation of alcohols over novel crystalline MoVO oxide. *Appl. Catal. A Gen.* **346**, 155–163. <https://doi.org/10.1016/j.apcata.2008.05.021> (2008).
- Li, J., Yang, Z., Li, S., Jin, Q. & Zhao, J. Review on oxidative desulfurization of fuel by supported heteropolyacid catalysts. *J. Ind. Eng. Chem.* **82**, 1–16. <https://doi.org/10.1016/j.jiec.2019.10.020> (2020).
- Huang, X. *et al.* Self-assembly of three Ag-polyoxovanadates frameworks for their efficient construction of CN bond and detoxification of simulant sulfur mustard. *Chin. Chem. Lett.* **33**, 2605–2610. <https://doi.org/10.1016/j.ccllet.2021.09.042> (2022).
- Yao, M.-Y., Liu, Y.-F., Li, X.-X., Yang, G.-P. & Zheng, S.-T. The largest Se-4f cluster incorporated polyoxometalate with high Lewis acid–base catalytic activity. *Chem. Commun.* **58**, 5737–5740. <https://doi.org/10.1039/D2CC01051H> (2022).
- Liu, Y.-F. *et al.* Self-assembly of a U(VI)-containing polytungstate tetramer with lewis acid–base catalytic activity for a dehydration condensation reaction. *Inorg. Chem.* **61**, 20358–20364. <https://doi.org/10.1021/acs.inorgchem.2c02918> (2022).
- Yang, G. *et al.* H4SiW12O40-catalyzed cyclization of epoxides/aldehydes and sulfonyl hydrazides: an efficient synthesis of 3,4-disubstituted 1H-pyrazoles. *Chin. Chem. Lett.* **33**, 1483–1487. <https://doi.org/10.1016/j.ccllet.2021.08.037> (2022).
- Yang, G. *et al.* Regio- and stereoselective synthesis of (Z)-3-ylidenephthalides via H3PMo12O40-catalyzed cyclization of 2-acylbenzoic acids with benzylic alcohols. *Chin. J. Chem.* **39**, 3017–3022. <https://doi.org/10.1002/cjoc.202100397> (2021).
- Yang, B., Pignatello, J. J., Qu, D. & Xing, B. Reoxidation of photoreduced polyoxotungstate ([PW12O40]4-) by different oxidants in the presence of a model pollutant kinetics and reaction mechanism. *J. Phys. Chem. A* **119**, 1055–1065 (2015).
- Sadjadi, S. & Heravi, M. M. Recent advances in applications of POMs and their hybrids in catalysis. *Curr. Org. Chem.* **20**, 1404–1444 (2016).
- Heravi, M. M. *et al.* A novel multi-component synthesis of 4-arylaminoquinazolines. *Tetrahedron Lett.* **50**, 943–945. <https://doi.org/10.1016/j.tetlet.2008.12.044> (2009).
- Samaha, S. & Majid, M. H. Recent advances in applications of POMs and their hybrids in catalysis. *Curr. Org. Chem.* **20**, 1404–1444. <https://doi.org/10.2174/1385272820666160216225330> (2016).
- Sadjadi, S., Tarighi, S., Moussavi, N. S. & Ahadi, N. Heteropolyacid supported on the composite of bentonite and ionic liquid containing acidic polymer: a highly selective catalyst for glycerol acetalization to solketal. *J. Mol. Struct.* **1256**, 132556. <https://doi.org/10.1016/j.molstruc.2022.132556> (2022).
- Mondal, J., Modak, A. & Bhaumik, A. Highly efficient mesoporous base catalyzed Knoevenagel condensation of different aromatic aldehydes with malononitrile and subsequent noncatalytic Diels–Alder reactions. *J. Mol. Catal. A Chem.* **335**, 236–241. <https://doi.org/10.1016/j.molcata.2010.11.039> (2011).
- Modak, A., Mondal, J. & Bhaumik, A. Porphyrin based porous organic polymer as bi-functional catalyst for selective oxidation and Knoevenagel condensation reactions. *Appl. Catal. A Gen.* **459**, 41–51. <https://doi.org/10.1016/j.apcata.2013.03.036> (2013).
- Bhanja, P., Kayal, U. & Bhaumik, A. Ordered mesoporous  $\gamma$ -Al<sub>2</sub>O<sub>3</sub> as highly efficient and recyclable catalyst for the Knoevenagel reaction at room temperature. *Mol. Catal.* **451**, 220–227. <https://doi.org/10.1016/j.mcat.2018.01.019> (2018).
- Sakthivel, B. & Dhakshinamoorthy, A. Chitosan as a reusable solid base catalyst for Knoevenagel condensation reaction. *J. Colloid Interface Sci.* **485**, 75–80. <https://doi.org/10.1016/j.jcis.2016.09.020> (2017).
- Rani, D., Singla, P. & Agarwal, J. ‘Chitosan in water’ as an eco-friendly and efficient catalytic system for Knoevenagel condensation reaction. *Carbohydr. Polym.* **202**, 355–364. <https://doi.org/10.1016/j.carbpol.2018.09.008> (2018).
- Nie, M. *et al.* Novel Pd/MOF electrocatalyst for hydrogen evolution reaction. *Mater. Chem. Phys.* **254**, 123481. <https://doi.org/10.1016/j.matchemphys.2020.123481> (2020).
- El-Shall, M. S. *et al.* Metallic and bimetallic nanocatalysts incorporated into highly porous coordination polymer MIL-101. *J. Mater. Chem.* **19**, 7625–7631. <https://doi.org/10.1039/B912012B> (2009).
- Hassan, H. M. A., Betiha, M. A., Mohamed, S. K., El-Sharkawy, E. A. & Ahmed, E. A. Salen- Zr(IV) complex grafted into amine-tagged MIL-101(Cr) as a robust multifunctional catalyst for biodiesel production and organic transformation reactions. *Appl. Surf. Sci.* **412**, 394–404. <https://doi.org/10.1016/j.apsusc.2017.03.247> (2017).
- Hassan, H. M. A., Betiha, M. A., Mohamed, S. K., El-Sharkawy, E. A. & Ahmed, E. A. Stable and recyclable MIL-101(Cr)-Ionic liquid based hybrid nanomaterials as heterogeneous catalyst. *J. Mol. Liq.* **236**, 385–394. <https://doi.org/10.1016/j.molliq.2017.04.034> (2017).
- Khder, A. E. R. S., Hassan, H. M. A. & El-Shall, M. S. Metal-organic frameworks with high tungstophosphoric acid loading as heterogeneous acid catalysts. *Appl. Catal. A Gen.* **487**, 110–118. <https://doi.org/10.1016/j.apcata.2014.09.012> (2014).
- Aljaddua, H. I., Alhumaimess, M. S. & Hassan, H. M. A. CaO nanoparticles incorporated metal organic framework (NH<sub>2</sub>-MIL-101) for Knoevenagel condensation reaction. *Arab. J. Chem.* **15**, 103588. <https://doi.org/10.1016/j.arabc.2021.103588> (2022).
- Goetjen, T. A. *et al.* Metal–organic framework (MOF) materials as polymerization catalysts: a review and recent advances. *Chem. Commun.* **56**, 10409–10418. <https://doi.org/10.1039/D0CC03790G> (2020).
- Li, P., Cheng, F.-F., Xiong, W.-W. & Zhang, Q. New synthetic strategies to prepare metal–organic frameworks. *Inorg. Chem. Front.* **5**, 2693–2708. <https://doi.org/10.1039/C8QI00543E> (2018).
- Gautam, S. *et al.* Metal oxides and metal organic frameworks for the photocatalytic degradation: A review. *J. Environ. Chem. Eng.* **8**, 103726. <https://doi.org/10.1016/j.jece.2020.103726> (2020).
- Mollabagher, H., Taheri, S., Mojtahedi, M. M. & Seyedmousavi, S. Cu-metal organic frameworks (Cu-MOF) as an environment-friendly and economical catalyst for one pot synthesis of tacrine derivatives. *RSC Adv.* **10**, 1995–2003. <https://doi.org/10.1039/C9RA10111J> (2020).
- Ali, M. *et al.* Recent advancements in MOF-based catalysts for applications in electrochemical and photoelectrochemical water splitting: A review. *Int. J. Energy Res.* **45**, 1190–1226. <https://doi.org/10.1002/er.5807> (2021).
- Dang, M.-H.D. *et al.* Effect of Fe(III)-based MOFs on the catalytic efficiency of the tandem cyclooxidative reaction between 2-aminobenzamide and alcohols. *New J. Chem.* **44**, 14529–14535. <https://doi.org/10.1039/D0NJ03136D> (2020).
- Lee, J.-H. *et al.* Functionalization of zirconium-based metal–organic frameworks for gas sensing applications. *J. Hazard. Mater.* **403**, 124104. <https://doi.org/10.1016/j.jhazmat.2020.124104> (2021).
- Dang, M.-H.D. *et al.* An effective combination of reusable Pd@MOF catalyst and deep eutectic solvents for high-performance C–C coupling reaction. *J. Ind. Eng. Chem.* **111**, 111–120. <https://doi.org/10.1016/j.jiec.2022.03.041> (2022).

36. Nguyen, L. H. T., Nguyen, T. T. T., Dang, M.-H.D., Tran, P. H. & Doan, T. L. H. Heterocyclic reaction induced by Brønsted-Lewis dual acidic Hf-MOF under microwave irradiation. *Mol. Catal.* **499**, 111291. <https://doi.org/10.1016/j.mcat.2020.111291> (2021).
37. Dang, M.-H.D. *et al.* Sulfate-functionalized hafnium-organic frameworks as a highly effective chemiresistive sensor for low-temperature detection of hazardous NH<sub>3</sub> gas. *Sens. Actuators B Chem.* **367**, 132094. <https://doi.org/10.1016/j.snb.2022.132094> (2022).
38. Sadjadi, S. & Koohestani, F. Palladated composite of MOF and cyclodextrin nanosponge: A novel catalyst for hydrogenation reaction. *J. Mol. Struct.* **1245**, 131068. <https://doi.org/10.1016/j.molstruc.2021.131068> (2021).
39. Zhong, Y., Wu, Z., Liu, X. & Li, L. Highly active rGO/Ca-MOF loaded Pd-M (M = Fe, Sb, Pb, Sn, Ag) composite catalysts towards ethylene glycol electrooxidation. *J. Electroanal. Chem.* **927**, 116970. <https://doi.org/10.1016/j.jelechem.2022.116970> (2022).
40. Heydari, A., Darroudi, M. & Lacić, I. Efficient N-sulfopropylation of chitosan with 1,3-propane sultone in aqueous solutions: Neutral pH as the key condition. *React. Chem. Eng.* **6**, 2146–2158. <https://doi.org/10.1039/D1RE00089F> (2021).
41. Zhao, Z.-S., Zhang, Y., Fang, T., Han, Z.-B. & Liang, F.-S. Chitosan-coated metal-organic-framework nanoparticles as catalysts for tandem Deacetalization-Knoevenagel condensation reactions. *ACS Appl. Nano Mater.* **3**, 6316–6320. <https://doi.org/10.1021/acsnm.0c01486> (2020).
42. Alleshagh, M., Sadjadi, S., Arabi, H., Bahri-Laleh, N. & Monflier, E. Palladated chitosan-halloysite bead as an efficient catalyst for hydrogenation of lubricants. *Mater. Chem. Phys.* <https://doi.org/10.1016/j.matchemphys.2021.125506> (2021).
43. Koohestani, F. & Sadjadi, S. Polyionic liquid decorated chitosan beads as versatile metal-free catalysts for catalyzing chemical reactions in aqueous media. *J. Mol. Liq.* <https://doi.org/10.1016/j.molliq.2021.115754> (2021).
44. Anbu, N., Hariharan, S. & Dhakshinamoorthy, A. Knoevenagel-Doebner condensation promoted by chitosan as a reusable solid base catalyst. *Mol. Catal.* **484**, 110744. <https://doi.org/10.1016/j.mcat.2019.110744> (2020).
45. Dhakshinamoorthy, A., Jacob, M., Vignesh, N. S. & Varalakshmi, P. Pristine and modified chitosan as solid catalysts for catalysis and biodiesel production: A minireview. *Int. J. Biol. Macromol.* **167**, 807–833. <https://doi.org/10.1016/j.ijbiomac.2020.10.216> (2021).
46. Hapiot, F., Bricout, H., Menuel, S., Tilloy, S. & Monflier, E. Recent breakthroughs in aqueous cyclodextrin-assisted supramolecular catalysis. *Catal. Sci. Technol.* **4**, 1899–1908. <https://doi.org/10.1039/C4CY00005F> (2014).
47. Menuel, S., Léger, B., Addad, A., Monflier, E. & Hapiot, F. Cyclodextrins as effective additives in AuNP-catalyzed reduction of nitrobenzene derivatives in a ball-mill. *Green Chem.* **18**, 5500–5509. <https://doi.org/10.1039/C6GC00770H> (2016).
48. Noël, S., Léger, B., Ponchel, A., Sadjadi, S. & Monflier, E. Cyclodextrins as multitask agents for metal nano-heterogeneous catalysis: A review. *Environ. Chem. Lett.* **19**, 4327–4348. <https://doi.org/10.1007/s10311-021-01298-5> (2021).
49. Silva, F., Caldera, F., Trotta, F., Nerin, C. & Domingues, F. C. Encapsulation of coriander essential oil in cyclodextrin nanospheres: A new strategy to promote its use in controlled-release active packaging. *Innov. Food Sci. Emerg. Technol.* **56**, 102177. <https://doi.org/10.1016/j.ifset.2019.102177> (2019).
50. Pawar, S., Shende, P. & Trotta, F. Diversity of  $\beta$ -cyclodextrin-based nanospheres for transformation of actives. *Int. J. Pharm.* **565**, 333–350. <https://doi.org/10.1016/j.ijpharm.2019.05.015> (2019).
51. Sadjadi, S., Heravi, M. M. & Malmir, M. Pd@HNTs-CDNS-g-C<sub>3</sub>N<sub>4</sub>: A novel heterogeneous catalyst for promoting ligand and copper-free Sonogashira and Heck coupling reactions, benefits from halloysite and cyclodextrin chemistry and g-C<sub>3</sub>N<sub>4</sub> contribution to suppress Pd leaching. *Carbohydr. Polym.* **186**, 25–34. <https://doi.org/10.1016/j.carbpol.2018.01.023> (2018).
52. Sadjadi, S., Heravi, M. M. & Raja, M. Composite of ionic liquid decorated cyclodextrin nanosponge, graphene oxide and chitosan: A novel catalyst support. *Int. J. Biol. Macromol.* **122**, 228–237. <https://doi.org/10.1016/j.ijbiomac.2018.10.160> (2019).
53. Xie, Q. *et al.* Effective adsorption and removal of phosphate from aqueous solutions and eutrophic water by Fe-based MOFs of MIL-101. *Sci. Rep.* **7**, 3316. <https://doi.org/10.1038/s41598-017-03526-x> (2017).
54. Sadjadi, S., Heravi, M. M. & Raja, M. Combination of carbon nanotube and cyclodextrin nanosponge chemistry to develop a heterogeneous Pd-based catalyst for ligand and copper free C-C coupling reactions. *Carbohydr. Polym.* **185**, 48–55. <https://doi.org/10.1016/j.carbpol.2018.01.020> (2018).
55. Sadjadi, S., Koohestani, F. & Heravi, M. M. Fabrication of a metal free catalyst for chemical reactions through decoration of chitosan with ionic liquid terminated dendritic moiety. *Sci. Rep.* **10**, 19666. <https://doi.org/10.1038/s41598-020-76795-8> (2020).
56. Wang, Y., Guo, W. & Li, X. Activation of persulfates by ferrocene-MIL-101(Fe) heterogeneous catalyst for degradation of bisphenol A. *RSC Adv.* **8**, 36477–36483. <https://doi.org/10.1039/C8RA07007E> (2018).
57. Sadjadi, S. & Koohestani, F. Synthesis and catalytic activity of a novel ionic liquid-functionalized metal-organic framework. *Res. Chem. Intermed.* <https://doi.org/10.1007/s11164-021-04565-w> (2021).
58. Mallik, S., Dash, S. S., Parida, K. M. & Mohapatra, B. K. Synthesis, characterization, and catalytic activity of phosphomolybdate supported on hydrous zirconia. *J. Colloid Interface Sci.* **300**, 237–243 (2006).
59. Luo, Z., Chen, H., Wu, S., Yang, C. & Cheng, J. Enhanced removal of bisphenol A from aqueous solution by aluminum-based MOF/sodium alginate-chitosan composite beads. *Chemosphere* **237**, 124493. <https://doi.org/10.1016/j.chemosphere.2019.124493> (2019).
60. Sadjadi, S., Koohestani, F., Mahmoodi, N. M. & Rabeie, B. Composite of MOF and chitin as an efficient catalyst for photodegradation of organic dyes. *Int. J. Biol. Macromol.* **182**, 524–533. <https://doi.org/10.1016/j.ijbiomac.2021.04.034> (2021).
61. Nalumsani, I., Birungi, G., Moodley, B. & Tebandeke, E. Preparation and identification of reduced phosphomolybdate via molybdenum blue reaction. *Orient. J. Chem.* <https://doi.org/10.13005/ojc/360403> (2020).
62. Mohammadi, A., Kazemeini, M. & Sadjadi, S. Synthesis and physicochemical evaluations of a novel MIL-101(Fe)-PMA-Biochar triple composite photocatalyst activated through visible-light and utilized toward degradation of organic pollutants: Optimal operations and kinetics investigations. *Photochem. Photobiol. Sci.* <https://doi.org/10.1007/s43630-023-00383-8> (2023).
63. Talebian-Kiakalaieh, A. & Tarighi, S. Synthesis of hierarchical Y and ZSM-5 zeolites using post-treatment approach to maximize catalytic cracking performance. *J. Ind. Eng. Chem.* **88**, 167–177. <https://doi.org/10.1016/j.jiec.2020.04.009> (2020).
64. Guibal, E. Heterogeneous catalysis on chitosan-based materials: A review. *Prog. Polym. Sci.* **30**, 71–109. <https://doi.org/10.1016/j.progpolymsci.2004.12.001> (2005).
65. Sadjadi, S., Akbari, M., Monflier, E., Heravi, M. M. & Leger, B. Pd nanoparticles immobilized on halloysite decorated with a cyclodextrin modified melamine-based polymer: A promising heterogeneous catalyst for hydrogenation of nitroarenes. *New J. Chem.* **42**, 15733–15742. <https://doi.org/10.1039/C8NJ03014F> (2018).
66. Hatefi-Ardakani, M., Saeednia, S., Pakdin-Parizi, Z. & Rafeezadeh, M. Efficient and selective oxidation of alcohols with tert-BuOOH catalyzed by a dioxomolybdenum(VI) Schiff base complex under organic solvent-free conditions. *Res. Chem. Intermed.* **42**, 7223–7230. <https://doi.org/10.1007/s11164-016-2531-x> (2016).
67. de Resende Filho, J. B. M., Pires, G. P., de Oliveira Ferreira, J. M. G., Teotonio, E. E. S. & Vale, J. A. Knoevenagel condensation of aldehydes and ketones with malononitrile catalyzed by amine compounds-tethered Fe<sub>3</sub>O<sub>4</sub>@SiO<sub>2</sub> nanoparticles. *Catal. Lett.* **147**, 167–180. <https://doi.org/10.1007/s10562-016-1916-1> (2017).
68. Miao, Z., Luan, Y., Qi, C. & Ramella, D. The synthesis of a bifunctional copper metal organic framework and its application in the aerobic oxidation/Knoevenagel condensation sequential reaction. *Dalton Trans.* **45**, 13917–13924 (2016).
69. Wang, D. & Li, Z. Bi-functional NH<sub>2</sub>-MIL-101(Fe) for one-pot tandem photo-oxidation/Knoevenagel condensation between aromatic alcohols and active methylene compounds. *Catal. Sci. Technol.* **5**, 1623–1628 (2015).
70. Toyao, T., Saito, M., Horiuchi, Y. & Matsuoka, M. Development of a novel one-pot reaction system utilizing a bifunctional Zr-based metal-organic framework. *Catal. Sci. Technol.* **4**, 625–628 (2014).

71. Aryanejad, S., Bagherzade, G. & Farrokhi, A. Efficient and recyclable novel Ni-based metal-organic framework nanostructure as catalyst for the cascade reaction of alcohol oxidation-Knoevenagel condensation. *Appl. Organomet. Chem.* **32**, 3995. <https://doi.org/10.1002/aoc.3995> (2018).
72. Yan, H., Zhang, H.-Y., Wang, L., Zhang, Y. & Zhao, J. Ru (OH) x supported on polyethylenimine modified magnetic nanoparticles coated with silica as catalyst for one-pot tandem aerobic oxidation/Knoevenagel condensation of alcohols and active methylene compounds. *React. Kinet. Mech. Catal.* **125**, 789–806 (2018).

### Acknowledgements

The authors appreciate the support of Iran Polymer and Petrochemical Institute, Al-zahra University, the Slovak Grant Agency VEGA under contract number 2/0140/20 and 2/0121/23, and the Slovak Research and Development Agency under contract number APVV-18-0480. This work is the result of the project implementation CEMBAM – Centre for Medical Bio-Additive Manufacturing and Research, ITMS2014+: 313011V358 and Advanced Bioactive Hydrogel Scaffolds for Regenerative Medicine (ABSACARM), ITMS2014+: 313011BWL6 supported by the Operational Programme Integrated Infrastructure funded by the European Regional Development Fund.

### Author contributions

S.S.: conceptualization; funding acquisition; project administration; resources; supervision; writing—review and editing. N.A.-D.: formal analysis; data curation; methodology; visualization; investigation; A.H.: resources; investigation; writing—original draft. M.H.: funding acquisition; resources; investigation.

### Competing interests

The authors declare no competing interests.

### Additional information

**Supplementary Information** The online version contains supplementary material available at <https://doi.org/10.1038/s41598-023-29548-2>.

**Correspondence** and requests for materials should be addressed to S.S. or M.M.H.

**Reprints and permissions information** is available at [www.nature.com/reprints](http://www.nature.com/reprints).

**Publisher's note** Springer Nature remains neutral with regard to jurisdictional claims in published maps and institutional affiliations.



**Open Access** This article is licensed under a Creative Commons Attribution 4.0 International License, which permits use, sharing, adaptation, distribution and reproduction in any medium or format, as long as you give appropriate credit to the original author(s) and the source, provide a link to the Creative Commons licence, and indicate if changes were made. The images or other third party material in this article are included in the article's Creative Commons licence, unless indicated otherwise in a credit line to the material. If material is not included in the article's Creative Commons licence and your intended use is not permitted by statutory regulation or exceeds the permitted use, you will need to obtain permission directly from the copyright holder. To view a copy of this licence, visit <http://creativecommons.org/licenses/by/4.0/>.

© The Author(s) 2023